Dynamic Analysis and Experimental Study of Direct-acting Centrifugal Speed Limiter

Xu Guo*, Yibo Wang**, Lianzhi Zhang*, Kun Yang*** and Fangzhou Zhu*

Keywords: Direct-acting centrifugal speed limiter, Dynamic analysis, Simulation analysis, Data processing, Experimental verification.

ABSTRACT

This paper introduces a direct-acting centrifugal speed limiter (DCSL) to address large braking errors and low sensitivity in ratchet-claw centrifugal speed limiters. A triggering model for the DCSL is established through dynamic analysis and simulated in MATLAB, revealing relationships between release speed, centrifugal block mass, speed regulating spring (SRS) stiffness, and SRS pre-compression. The DCSL mathematical model is derived and validated via ADAMS dynamic simulation. An experimental platform is built, and MATLAB models experimental data, confirming the mathematical model's reliability with errors between 0.11% and 8.89%. The DCSL exhibits fast response and a wide speed limitation range, offering a new design approach for highsensitivity, low-error centrifugal speed limiters.

INTRODUCTION

In recent years, with the acceleration of China's urbanization process, the growth of the global population, and the improvement of people's requirements for convenience of life, the number of building elevators has also been growing rapidly (Wang, 2020; Gao, 2014). By the end of 2019, there

Paper Received December, 2024. Revised March, 2025. Accepted March, 2025. Author for Correspondence: Yibo Wang.

were about 20 million elevators worldwide, 7.0975 million in China, accounting for 35 % (ShuangChang, 2020). The number of elevators in China increased by 700,000 every year. China's elevator ownership, annual production, and annual growth are the world's first (DING Caihong, 2021). However, there are many security risks behind the huge elevator market. The elevators in China generally have the use of large passenger flow and high load, and the elevator safety situation is becoming more and more serious (Shuangchang, 2020). Although engineers and technicians continue to improve the safety performance of traction elevators, there are often accidents of elevators in buildings where the elevators are speeding up to the top or falling out of control (Yanbin, 2020). In 2022, a total of 108 special equipment accidents and related accidents occurred nationwide, with 101 deaths. Compared with 2021, the number of accidents decreased by 2, a decrease of 1.82 %, and the number of deaths increased by 2, an increase of 2.02 % (China Special Equipment Safety, 2023). It can be seen that although the number of elevator accidents is relatively small, in the event of an accident, the property damage and personal injury caused by it are very serious (Prahlow, 2020). It is worth noting that similar accidents not only occur in the elevators used in daily life but also often occur in the auxiliary transportation of coal mines and the cages used for carrying people and materials in mining enterprises. By the end of 2019, the elevator fault record of an elevator enterprise was 5761, which was composed of its own component fault and external factor fault. Among them, there were 4383 failures of its components, accounting for 76.1 % of the total number of repair failures. There were 1378 external faults, accounting for 23.9 % of the total number of repair faults (Yanbin, 2020).

As an important safety component of an elevator and cage, the speed limiter can monitor its running speed (Chen, 2016). When the running speed of the elevator or cage exceeds a certain value, the speed limiter can monitor the abnormal speed in time, and then trigger the braking system through its mechanical

^{*} Graduate Student, College of Mechanical Engineering and Automation, Liaoning University of Technology, Jinzhou, 121000, China

^{**} Lecturer, College of Mechanical Engineering and Automation, Liaoning University of Technology, Jinzhou, 121000, China.

^{***} Associate Professor, College of Mechanical Engineering and Automation, Liaoning University of Technology, Jinzhou, 121000, China.

structure, so that the elevator or cage can be stopped to avoid stalling and causing accidents. According to the action principle, it can be divided into pendulum type and centrifugal type (Yang, 2015). The centrifugal speed limiter has a wide range of speed applications. It has good stability and reliability under various working conditions and is widely used in industrial applications. Cheng-Chi Wang (2024) used the maximum Lyapunov exponent data of bearing number and rotor mass to distinguish the stability of the rotor in double circumferential slots air bearing system very precisely. Ta-Jen Peng (2024) developed a new model that can be effectively used to predict the Symmetric Aerostatic Cavities Bearing system and prevent nonlinear behavior from occurring, thereby avoiding the damage and deformation of the high rotational speed rotor resulting from bearing instabilities. [13] Wang Aerospatiale designed a centrifugal regulator to control the unfolding rate of the deployable element, which has been manufactured and tested for IUE solar cell arrays. Michael J. Gradziel (2008) studied a compact lowering device on a rover, which can use a centrifugal friction brake to issue a tether at a stable speed to reduce the payload.

Usually, the centrifugal speed limiter is the most widely used type of speed limiter at present. However, the ratchet-claw mechanism is widely used in its trigger mechanism. When the speed limiter reaches the release speed, the claw may drive the ratchet wheel to rotate for one week before triggering the braking system. The ratchet wheel rotates for one week, which will cause the elevator to slide down as much as 1m ~ 3m distance, which will greatly affect the safety of the elevator. Given the above problems and actual needs, this paper designs a direct-acting centrifugal speed limiter (DCSL) with small braking errors and high sensitivity. By establishing the dynamic model of the DCSL and analyzing the motion of the key components, the trigger model of the DCSL is deduced according to the analysis results. The simulation analysis is carried out by MATLAB to study the relationship and variation law between the parameters, and the working conditions and parameter values of the DCSL are set. The mathematical model of the DCSL is obtained by theoretical calculation.

STRUCTURAL DESIGN

Structure of DCSL

The DCSL designed in this paper is mainly composed of a speed limiter box, consecutive board, trigger shaft, T- plate, centrifugal block, and speed regulating spring (SRS) components. Among them, the two T-type pressure plates are symmetrically arranged and connected with the centrifugal block through bolts respectively. Under the premise of emergency braking, the technical problems of the current centrifugal DCSL are effectively solved, and the safety of passengers and

equipment can be better guaranteed. Figure 1 is a schematic diagram of the structure of the DCSL.

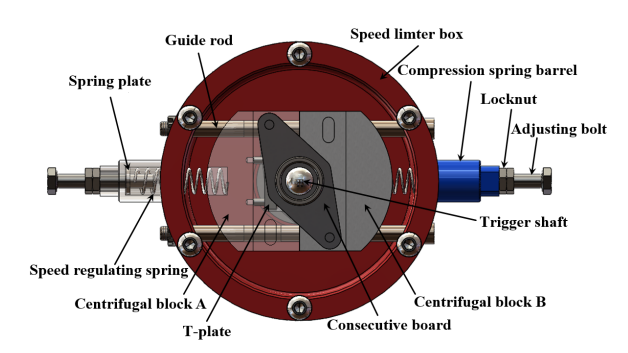


Fig.1. Schematic diagram of the structure of the DCSL.

The Working Principle of the DCSL System

The DCSL is designed according to the relationship between centrifugal force and rotational speed. The DCSL is coaxially installed with a speed measuring wheel (SMW). The DCSL and the SMW are connected by a flat key. In the work, the SMW drives the speed limiter to rotate. On the DCSL, the two centrifugal blocks are symmetrically arranged and connected to each other through the connecting board, which can move along the two guide rods relative to the DCSL. The head of the two centrifugal blocks has a groove with a SRS installed inside, and the SRS is installed inside. When the DCSL works normally, the spring compression force makes the centrifugal block keep tensioning to the shaft center of the DCSL, and the compression force of the SRS can be adjusted by the outer adjusting bolt. When the elevator car or cage runs normally, the DCSL rotates at a uniform speed under the drive of the coaxial SMW. Under the mutual balance of the compression force of the SRS and the centrifugal effect, the centrifugal block maintains a certain distance from the DCSL, and rotates with the DCSL. The tail lock tongue of the two T-plates is located in the trigger shaft groove to ensure that the trigger shaft does not move axially, and the DCSL runs normally and stably. Figure 2 is the full view of the DCSL.

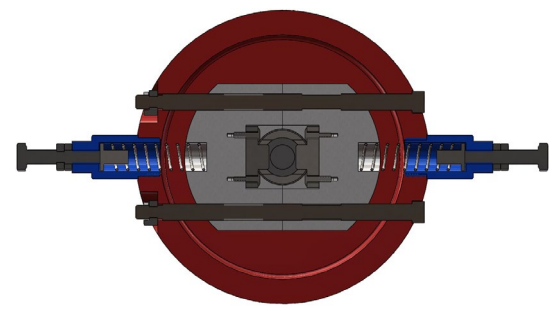
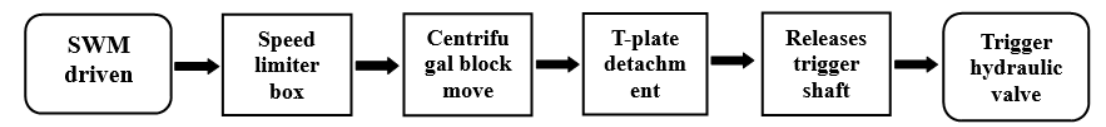


Fig.2. Full-section view of DCSL.

When the running speed of the elevator car or cage exceeds the preset speed, that is, when the speed increases, the centrifugal effect of the centrifugal block is more obvious, and the stable state of the tension force of the SRS is broken. The guide rod moves outward away from the axis of the DCSL, and the distance from the axis of the DCSL increases. At the same time, the centrifugal force makes the T-shaped pressure plate of the same part as the centrifugal block move accordingly. The tail lock tongue of the T-plate overcomes the friction between the trigger shaft and the trigger shaft, releases the trigger shaft, and then triggers the hydraulic valve, starts the hydraulic brake system to stop the elevator car or cage, and realizes the speed monitoring. The working process of the DCSL is shown in Figure 3.



The working flow chart of each mechanism when the DCSL is triggered.

Dynamics Analysis and Mathematical Model

For the convenience of analysis, the centrifugal force of other parts except the centrifugal block is not considered in the whole movement process. On the DCSL, the inner and outer surfaces of the two centrifugal blocks have connecting boards connecting the two centrifugal blocks respectively, and the two connecting boards are symmetrical about the center of the DCSL axis. It can be seen that during the movement of the DCSL, the two connecting boards produce the same size and opposite direction of the couple, that is, the generated rotation effects cancel each other out, so the problem of the connecting board generating the couple when the DCSL is triggered is not considered. The dynamic model of the DCSL is shown in Figure 4.

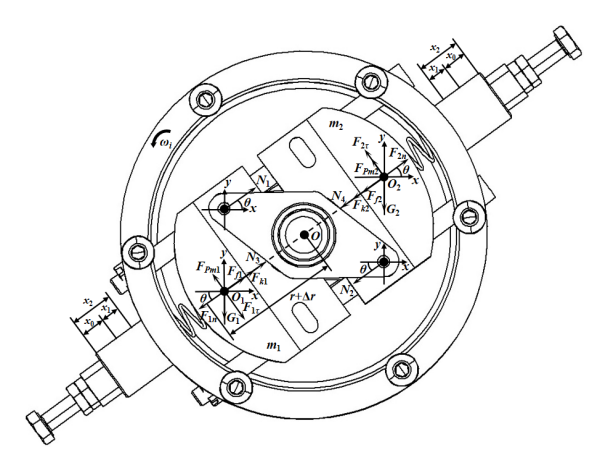


Fig. 4. Dynamic model of DCSL.

Motion Analysis of Centrifugal Block Components

Because the DCSL is driven by the speed wheel through the flat key connection and rotates at a constant speed, the angular speed ω of the speed wheel is equal to the angular speed ω_i of the DCSL,

$$\omega = \frac{V}{R_1} = \omega_i,\tag{1}$$

Where: V is the center-of-mass velocity of the speed

wheel; R_1 is the radius of the speed wheel;

When the DCSL speed reaches the critical value v_{cri} , the two centrifugal blocks simultaneously have a small radial displacement Δr along the guide rod and trigger a further compression of the SRS by x_1 displacements with the following relationship:

$$R = r + \Delta r,\tag{2}$$

Where: \mathbf{r} is the distance from the center of the DCSL shaft to the center of mass of the centrifugal block when the DCSL is not triggered; \mathbf{R} is the distance from the center of the DCSL shaft to the center of mass of the centrifugal block when the DCSL is released from the trigger shaft;

The centrifugal block rotates in the DCSL, so the angular velocity of the DCSL is:

$$\omega_i = \frac{v_0}{R} = \frac{v_{cri}}{R} = \frac{v_{cri}}{r + \Delta r},\tag{3}$$

Where: v_0 is the linear velocity of the centrifugal block center of mass; v_{cri} is the critical linear velocity of the trigger shaft by the release of the DCSL;

Assuming that the movement of the DCSL is very stable, regardless of the vibration impact, the movement of the centrifugal block in a very short time is a uniform process, with normal acceleration and tangential acceleration:

$$a_n = \omega_i^2 R = \omega_i^2 (r + \Delta r), \tag{4}$$

$$a_n = \omega_i^2 R = \omega_i^2 (r + \Delta r), \tag{4}$$

$$a_\tau = R\varepsilon = R \frac{d\omega_i}{dt} = (r + \Delta r)\varepsilon, \tag{5}$$
Because the DCSL is a constant speed

process, ω_i is constant, the tangential acceleration is zero, and the normal centrifugal force is:

$$F_{1n} = m_1 \omega_i^2 R = m_1 \omega_i^2 (r + \Delta r), \tag{6}$$

$$F_{1n} = m_1 \omega_i^2 R = m_1 \omega_i^2 (r + \Delta r),$$

$$F_{2n} = m_2 \omega_i^2 R = m_2 \omega_i^2 (r + \Delta r),$$
(6)

When the rotational speed of the DCSL exceeds the limited speed, the centrifugal block moves outward away from the center of the shaft under the action of centrifugal force, and at the same time, the centrifugal force makes the T-plate connected with the centrifugal block through the bolt connection to be an integral part of the T- plate moves along with it, the T-plate breaks away from the trigger shaft slot position, and there is friction between the tail part of the T-plate and the trigger shaft F_f , that is:

$$F_{f1} = \mu F_{P1},\tag{8}$$

$$F_{f2} = \mu F_{P2},\tag{9}$$

Where: μ is the friction coefficient between the end of the T-plate lever and the trigger shaft; F_{P} is the positive pressure between the end of the T-plate lever and the trigger shaft;

Because the two centrifugal blocks are symmetrically arranged and the mass is equal, the two speed regulating springs are the same, and the space length of the SRS installed in the DCSL is certain. Therefore, when the SRS is selected according to the working requirements, the difference between the free length and the installation space length will cause the SRS to preload the centrifugal block N, that is:

$$N_3 = k(L_1 - L_2), (10)$$

$$N_4 = k(L_1 - L_2), (11)$$

Where: k is the spring stiffness of the SRS; L_1 is the free length of the SRS; L_2 is the length of the installation space of the SRS;

When the DCSL releases the trigger shaft, the two centrifugal blocks move x_1 displacement along the guide rod, and the SRS is further compressed, according to Hooke's law:

$$F_{k1} = kx_2 = k(x_0 + x_1), (12)$$

$$F_{k1} = kx_2 = k(x_0 + x_1), \tag{13}$$

 $F_{k1} = kx_2 = k(x_0 + x_1),$ (12) $F_{k1} = kx_2 = k(x_0 + x_1),$ (13) Where: F_k is the compression force of the SRS; x_0 is the pre-compression amount of the SRS; x_1 is the compression amount of the SRS;

Assuming that there is no error when the two centrifugal blocks move outward along the direction of the guide rod away from the axis, the supporting force of the connecting board on the two centrifugal blocks is equal and zero, that is:

$$N_1 = N_2 = 0, (14)$$

Due to the smooth movement of the DCSL, omitted due to slight vibration on the movement of the system; also omitted from the movement of the DCSL air resistance and friction and other factors on the movement of the system; ignoring the mass of the connecting rod, $G_3 = 0$; when the centrifugal block A movement to reach equilibrium, a strong balance equation:

$$\sum_{i} F_{x} = 0: F_{1n} \cos \theta + F_{Pm1} \sin \theta - N_3 \cos \theta - F_{k1} \cos \theta - F_{f1} \cos \theta = 0,$$

$$(15)$$

$$\sum Fy = 0: F_{1n}\sin\theta + G_1 - F_{Pm1}\cos\theta - N_3\sin\theta - F_{k_1}\sin\theta - F_{f_1}\sin\theta = 0,$$
(16)

Where: F_{pm1} is the positive pressure of the guide rod on the centrifugal block A;

Simplify Eq. (15):

$$F_{Pm1} = N_3 \frac{\cos \theta}{\sin \theta} + F_{k1} \frac{\cos \theta}{\sin \theta} + F_{f1} \frac{\cos \theta}{\sin \theta} - F_{1n} \frac{\cos \theta}{\sin \theta}, (17)$$

The equation can be obtained by substituting the above formula into formula (16), and the equation is merged and simplified, that is:

$$F_{1n} + G_1 \sin \theta - N_3 - F_{k1} - F_{f1} = 0, \tag{18}$$

Substituting the specific expressions of the parameters acting on the centrifugal block A, we obtain: $m_1\omega_i^2(r+\Delta r) + m_1g\sin\theta - k(L_1-L_2) - k(x_0 +$

$$x_1) - \mu F_{P1} = 0, (19)$$

The force equilibrium equation for the centrifugal block B is similarly obtained, that is:

$$\sum Fx = 0: F_{2n}\cos\theta - F_{Pm2}\sin\theta - N_4\cos\theta - F_{k2}\cos\theta - F_{f2}\cos\theta = 0,$$
(20)

$$F_{k2}\cos\theta - F_{f2}\cos\theta = 0, \qquad (20)$$

$$\sum Fy = 0: F_{2n}\sin\theta + F_{pm2}\cos\theta - G_2 - N_4\sin\theta - F_{k2}\sin\theta - F_{f2}\sin\theta = 0, \qquad (21)$$

To simplify the formula (20), there are:
$$F_{Pm2} = F_{2n} \frac{\cos \theta}{\sin \theta} - N_4 \frac{\cos \theta}{\sin \theta} - F_{k2} \frac{\cos \theta}{\sin \theta} - F_{f2} \frac{\cos \theta}{\sin \theta}$$
(22)

The equation can be obtained by substituting the above formula into formula (21), and the equation is merged and simplified, that is:

$$F_{2n} - G_2 \sin \theta - N_4 - F_{k2} - F_{f2} = 0, \tag{23}$$

 $F_{2n} - G_2 \sin \theta - N_4 - F_{k2} - F_{f2} = 0,$ (23) Substituting the specific expressions of the parameters acting on the centrifugal block B, we obtain: $m_2\omega_i^2(r+\Delta r) - m_2g\sin\theta - k(L_1-L_2) - k(x_0+L_1-L_2)$ $x_1) - \mu F_{P2} = 0,$

Combining Equation (19) and Equation (24), the total force balance equation of the two centrifugal blocks when the DCSL releases the trigger shaft is:

$$(m_1 + m_2)\omega_i^2(r + \Delta r) + (m_1 - m_2)g\sin\theta = 2k(L_1 - L_2 + x_0 + x_1) + \mu(F_{P_1} + F_{P_2}),$$
(25)

Since the mass of the two centrifugal blocks is taken to be the same value, $m_1 = m_2$, due to the consideration of gravitational equilibrium of the DCSL,

$$(m_1 + m_2)\omega_i^2(r + \Delta r) = 2k(L_1 - L_2 + x_0 + x_1) + \mu(F_{P_1} + F_{P_2}),$$
(26)

Motion Analysis of T- plate

In practical applications, the outer end of the trigger shaft of the DCSL is coaxially installed with a proximity switch (NPN normally closed) hydraulic sensor. The pre-tightening spring of the hydraulic sensor is installed in front of the sensor. When the DCSL works normally, the pre-tightening spring applies an appropriate pre-tightening force to the outer end of the trigger shaft through the push rod to ensure the normal operation of the DCSL. The trigger shaft compression spring is installed at the inner end of the trigger shaft of the DCSL. When the trigger shaft is installed, a certain amount of displacement needs to be compressed to clamp the T-plate. When the DCSL works normally, because the preload of the preload spring of the hydraulic sensor is greater than the compression force of the compression spring of the trigger shaft, the T-plate is in the position of the trigger shaft slot, so the trigger shaft will not move axially. When the centrifugal force of the centrifugal block is less than the tension force of the SRS, there will be no radial displacement. When the centrifugal force of the centrifugal block is greater than the tension force of the SRS, that is, the centrifugal block breaks the stable state of the tension force of the SRS and moves away from the axis. The T- plate is then removed from the position of the trigger shaft groove. The trigger shaft will move along the axial direction to the inside of the DCSL under the action of the preload spring preload. The trigger shaft compression spring is further compressed. The hydraulic sensor receives the signal, triggers the hydraulic valve and starts the hydraulic braking system. As mentioned earlier, this is analyzed according to Figure 5, with the following:

$$F_{k3} = k_3 x_3, (27)$$

Where: F_{k3} is the preload force of the hydraulic sensor preload spring acting on the outer face of the trigger

shaft; k_3 is the spring stiffness of the hydraulic sensor preload spring; x_3 for the hydraulic sensor preload spring total compression;

$$F_{k4} = k_4 x_4, \tag{28}$$

Where: F_{k4} for the trigger shaft compression spring compression force acting on the inner end face of the trigger shaft; k_4 for the trigger shaft compression spring stiffness; x_4 for the trigger shaft compression spring total compression;

$$F_{P1} + F_{P2} = F_{k3} - F_{k4} = k_3 x_3 - k_4 x_4, \tag{29}$$

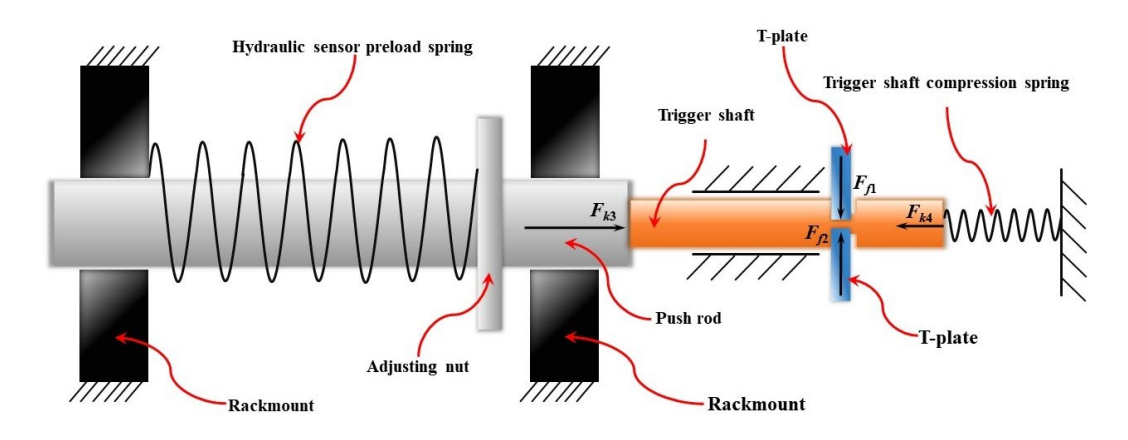


Fig.5. T-plate action force analysis diagram.

From the above analysis, the trigger model equation of the DCSL can be established as follows:

$$(m_1 + m_2)\omega_i^2(r + \Delta r) = 2k(L_1 - L_2 + x_0 + x_1) + \mu(k_3x_3 - k_4x_4),$$
 (30)

In summary, the relationship equation between the pre-compression of the SRS and the angular velocity of the DCSL, the stiffness of the SRS and the mass of the centrifugal block is:

$$x_0 = \frac{1}{2k} [(m_1 + m_2)\omega_i^2(r + \Delta r) - \mu(k_3 x_3 - k_4 x_4)] - (L_1 - L_2 + x_1),$$
(31)

where x_3 and x_4 are ultimately determined by the travel of the hydraulic sensor preload spring and the trigger shaft compression spring during operation, and x_1 is determined by the small displacement Δr of the centrifugal block movement, which can usually be approximated as equal (Li Jun, 2020).

Dynamic Model Simulation Analysis

Based on the above-mentioned DCSL trigger model, the known parameters are input, and the model simulation calculation is performed using MATLAB. The total mass of the centrifugal block $M=m_1+m_2$, the stiffness of the SRS and the pre-compression

of the SRS x_0 are selected as the main variables (LI Wanli, 2017). Because the DCSL adopts high-quality materials such as high-quality carbon structural steel or alloy wear-resistant steel, and heat treatment is carried out on key parts, the friction coefficient is μ =0.1under non-lubricated working conditions. Without considering the friction except the T-plate, the simulation parameters are set to take the following values respectively: $r+\Delta r$ =26.97mm, x_1 =2.5mm, L_1 =50.8mm, L_2 =41.54mm, k_3 =2.305N/mm, x_3 =10mm, x_4 =1.173N/mm, x_4 =14.25 mm.

The total mass of the centrifugal block and the stiffness of the SRS are taken as the research variables. The value range of the total mass of the centrifugal block is set to be $0.3 \sim 1.8 {\rm kg}$, and the value range of the stiffness of the SRS is $0 \sim 3000 {\rm N/m}$. When the precompression of the SRS is constant at $0.01 {\rm m}$, the relationship between the release speed of the DCSL, the total mass of the centrifugal block and the stiffness of the SRS is shown in Figure 6. The simulation results show that with the increase of the stiffness of the SRS and the decrease of the total mass of the centrifugal block, the release speed of the DCSL increases gradually, and the stiffness of the SRS has a greater influence on the change range of the release speed of the DCSL than the total mass of the centrifugal block.

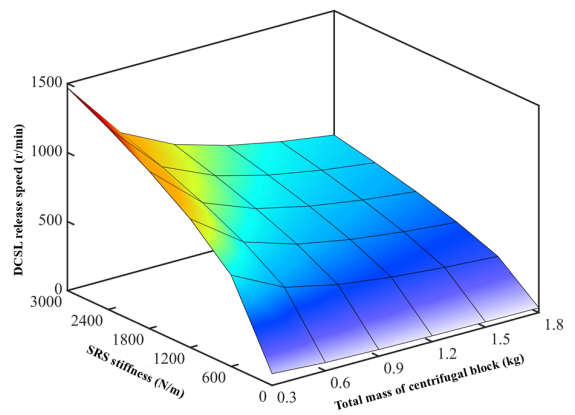


Fig. 6. The relationship between the total mass of the centrifugal block, the stiffness of the SRS and the release speed of the DCSL.

Taking the pre-compression of the SRS and the stiffness of the SRS as the research variables, the range of the pre-compression of the SRS is set to be 0 \sim 0.01m, and the range of the stiffness of the SRS is set to be 0 \sim 3000N/m. When the total mass of the centrifugal block is 1.2kg, the relationship between the release speed of the SRS, the pre-compression of the SRS and the stiffness of the SRS is shown in Figure 7. The simulation results show that with the increase of the pre-compression of the SRS and the increase of the stiffness of the SRS, the release speed of the DCSL also increases gradually.

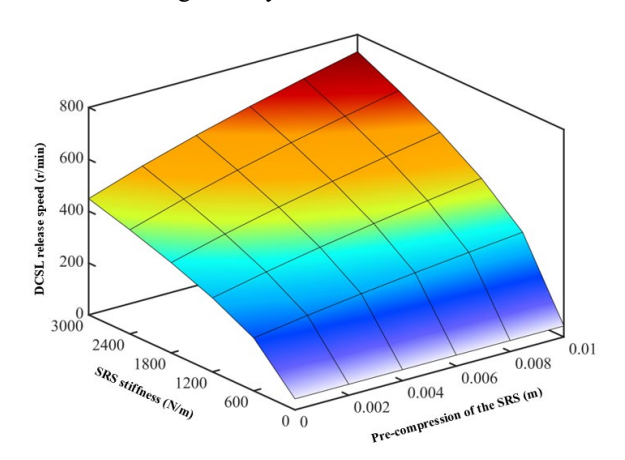


Fig. 7. The relationship between the precompression of the SRS, the stiffness of the SRS and the release speed of the DCSL.

The total mass of the centrifugal block is taken as the research variable, and the total mass of the centrifugal block is set to 0.3,0.6,0.9,1.2,1.5,1.8 kg respectively, and the value range of the stiffness of the SRS is $0 \sim 3000$ N/m. When the pre-compression of the SRS is taken as a constant value of 0.01m, the simulation results show that under the same stiffness of the SRS, the greater the total mass of the centrifugal block, the smaller the release speed of the DCSL, as shown in Figure 8.

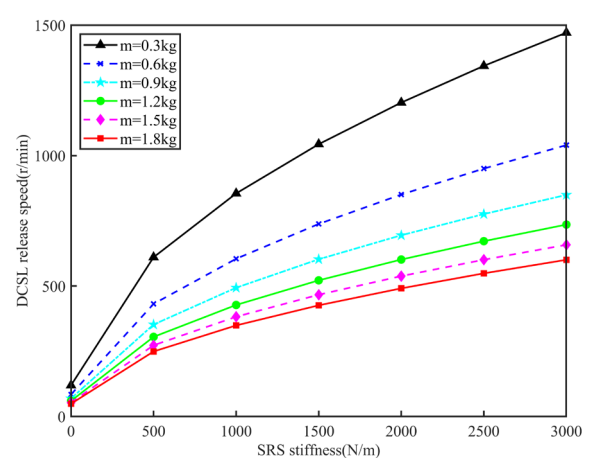


Fig.8. Relationship between release speed of DCSL and total mass of centrifugal block.

The pre-compression of the SRS is taken as the research variable, and the pre-compression of the SRS is set to 0,0.002,0.004,0.006,0.008,0.01m respectively. The value range of the SRS stiffness is $0 \sim 3000$ N/m. When the total mass of the centrifugal block takes a constant value of 1.2 kg, the simulation results show that under the same stiffness of the SRS, the greater the pre-compression of the SRS, the greater the release speed of the DCSL, as shown in Figure 9.

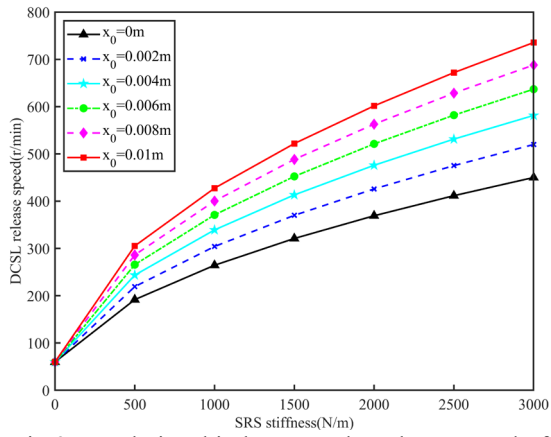


Fig.9. Relationship between the release speed of DCSL and the pre-compression of the SRS.

Establishment of Mathematical Model

Take the above DCSL kinetic analysis model as the theoretical basis to set the working conditions: speed wheel center-of-mass linear velocity V = 4.8 m/s, speed wheel diameter $D_1 = 280 \text{mm}$, the radius of the speed wheel $R_1 = 140 \text{mm}$, then the angular velocity of the speed wheel ω is:

velocity of the speed wheel
$$\omega$$
 is:

$$\omega = \frac{V}{R_1} = \frac{4.8m/s}{0.14m} = 34.29 rad/s = \omega_i, \quad (32)$$

That is, the DCSL angular velocity ω_i =34.29rad/s, which is converted into a rotational speed of 327.61r/min, so when the DCSL rotational speed reaches this value, the DCSL should be triggered

in time to release the trigger shaft to start the hydraulic braking system. Set the braking speed error does not exceed 10%, then the mathematical model is established.

From the analysis results in the previous subsection, it can be seen that the SRS stiffness and SRS pre-compression is proportional to the DCSL release speed, the total mass of the centrifugal block and the DCSL release speed is inversely proportional to the relationship, and the stiffness of the SRS is greater than the total mass of the centrifugal block on the DCSL release speed change amplitude of the impact, so the two centrifugal block mass is set to take the same value of 0.6kg. Because of the measurement of the DCSL to release the triggering axis SRS Compression $x_1 = 2.5 \text{mm}$, taking into account the DCSL range should be increased as much as possible to meet the requirements of more working conditions, the preliminary selection of SRS pre-compression $x_0 = 2$ mm, then through the formula (31) and the working conditions of the DCSL angular speed can be calculated SRS stiffness k, so that the SRS precompression is the main variable, the design of the experiment only need to discuss the different SRS precompression DCSL can be in the specified brake speed error range to reach the DCSL. When designing the experiment, it is only necessary to discuss whether the DCSL can reach the release speed of the DCSL within the specified braking speed error range with different precompression of the DCSL spring. According to the structural size requirements of the DCSL, through the query mechanical design manual, determine the inner diameter, outer diameter and free length of the SRS, you can determine the parameters of the SRS, so the free length of the SRS L_1 = 50.8mm, the length of the installation space of the SRS is:

$$L_2 = 41.54mm - 2mm = 39.54mm, \quad (33)$$

In the formula, when the adjusting bolt is not adjusted, i.e., when the pre-compression of the SRS $x_0 = 0$ mm, the length of the mounting space of the SRS is 41.54mm at the maximum value.

Substitute the above parameters into the equation (31), calculated k = 1.187 N/mm, by querying the mechanical design manual and in order to increase the DCSL range as much as possible, select the SRS stiffness k = 1.218 N/mm, through the calculation of the DCSL angular speed $\omega_i = 34.72 \text{rad} / \text{s}$, and the working conditions of the angular velocity required by the error of 1.25% to meet the design requirements of the foreseen, i.e. The mathematical model is established.

In summary, according to the parameter setting of the DCSL, the angular velocity of the DCSL can be calculated by Equation (31) with different precompression of the SRS, which is converted to rotational speed as shown in Table 1.

Table 1. Theoretical release speed table for DCSL.

Pre-compression(mm)	Theoretical release speed (r/min)
0	287.38
1	310.37
2	331.77
3	351.87
4	370.88
5	388.96
6	406.24
7	422.82
8	438.77
9	454.16
10	469.04

ADAMS DYNAMICS SIMULATION ANALYSIS

Simulation Model Establishment

For the relatively complex three-dimensional model of the DCSL, it is very difficult to establish it in ADAMS software, so the three-dimensional model is established by using the three-dimensional software SolidWorks. According to the above mathematical model, the three-dimensional model of the DCSL is established by SolidWorks under the same parameter setting, and the structure of the model is simplified. It is saved as a format compatible with ADAMS and imported into ADAMS simulation software for analysis. The imported DCSL model is shown in Figure 10, which is mainly composed of speed limiter box, guide rod, compression spring barrel, two centrifugal blocks and T- plate (Zhang Shuai, 2024).

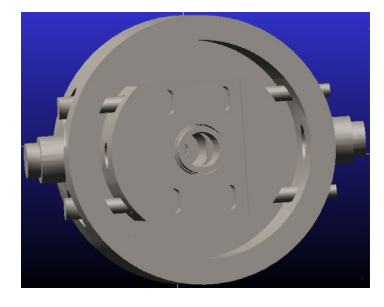


Fig. 10. Simulation model of DCSL.

By defining the quality attribute information of the model, constraints are imposed on each part of the model according to the actual connection situation. The constraints of important parts are shown in table 2.

T 11 A	C '.' 1	4	
Table /	(rifical	component	constraints.
rabic 2.	Critical	component	constraints.

Campaign subtitle	Typology	Part 1	Part 2
JOINT_1	Stationary sub	tachymeter shaft	Ground
JOINT_2	Rotating sub	Speed Limiter Box	Tachymeter shaft
JOINT_3	Stationary sub	Guide rod 1	Speed Limiter Box
JOINT_4	Stationary sub	Guide rod 2	Speed Limiter Box
JOINT_5	Mobile sub	Centrifuge block 1	Guide rod 1
JOINT_6	Mobile sub	Centrifuge block 1	Guide rod 2
JOINT_7	Mobile sub	Centrifuge block 2	Guide rod 1
JOINT_8	Mobile sub	Centrifuge block 2	Guide rod 2

Add the SRS between the compression spring barrel slot and the centrifugal block slot on both sides of the DCSL, the active object is the centrifugal block, the passive object is the speed limiter box, and the stiffness coefficient is selected to be 1.218, i.e., the stiffness of the SRS k = 1.218N/mm. due to the existence of a difference between the free length of the SRS and the length of the mounting space, there is a preload of the SRS to the centrifugal block when the spring is added, which is calculated as 13.71468N by the equation (10) and the equation (11) is calculated as $N_3 = N_4 = 13.71468$ N. Because the trigger mechanism is simplified in the simulation model to visualize the results, the positive pressure exerted on the T-plate is counted into the total preload of the SRS, i.e., the centrifugal block needs to break the tension of the SRS and the total preload before releasing the trigger axle, which is consistent with the trigger model in Section II. The total preload is obtained as 20.04943 by using Eq. (29) with the above mentioned, therefore, the two SRS parameters are set separately after adding the two SRS in ADAMS.

The reliability of the collision contact problem

of the DCSL in the simulation is ensured by setting the contact between the centrifugal block A and the speed limiter box, centrifugal block B and the speed limiter box, and centrifugal block A and centrifugal block B. In the contact, the entity-to-entity is selected the default normal force parameter is used and the friction is set to none.

The STEP function is used in the drive part to define the rotational speed, from the working conditions set above, it is known that the release angular speed of the DCSL should be 34.29 rad/s, and the error of braking rotational speed is 10%, so the function is defined as STEP(time, 0, 0, 10, -34.29), this STEP function defines a linear change process from time 0s to 10s, in which the rotational speed increases from 0rad/s to -34.29rad/s. In the function time is the current time variable, which changes as the simulation progresses. During the process, the rotational speed increases from 0 rad/s to -34.29 rad/s. In the function, time is the current time variable, which changes as the simulation progresses. When the rotational speed increases linearly from 0 rad/s at time=0s to -34.29 rad/s at time=10s, the rotational speed is negative, indicating that the object is doing counterclockwise rotation, which is consistent with the dynamics model in Section 2.

Analysis of Simulation Results

Set the termination time as 10s, and the number of simulation steps as 10000, after the completion of the simulation in the ADAMS post-processing module to get a series of parameter change curves of the DCSL. Because the DCSL releases the trigger axis when the speed spring compression = 2.5mm, so in the DCSL post-processing module, select the object for the force in the SPRING_1 and SPRING_2 deformation to draw the curve, that is, the observation of the two-SRS compression of the change in the amount, as shown in Figure 11.

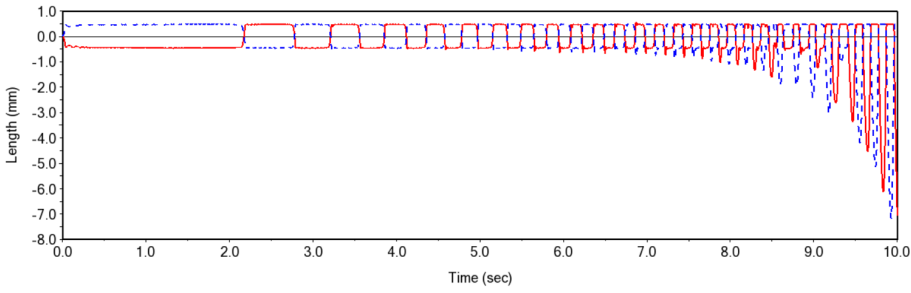


Fig. 11. Simulated compression of SRS.

As can be seen from the above figure, when time=9.19s one of the speed spring compression has exceeded 2.5mm, but the two SRS have not reached the position of both out of the slot of the trigger shaft. When time=9.48s, the compression of both SRS

exceeds 2.5mm, so the trigger shaft is successfully released. At this time, select CM_Angular_Velocity. Mag through the body of the object to view the angular velocity trend of the two centrifugal blocks, as shown in Figure 12.

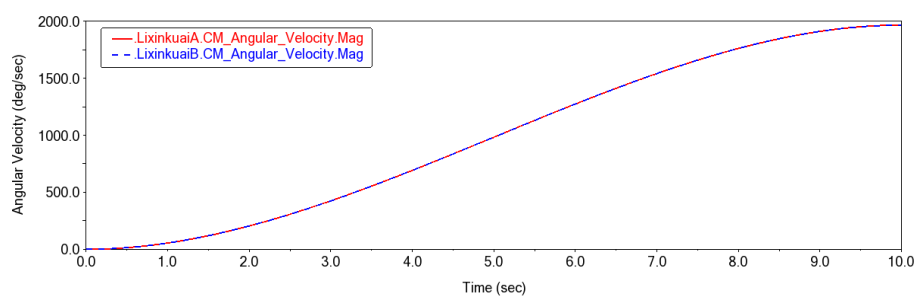


Fig. 12 Plot of angular velocity variation of centrifugal block.

As can be seen from Figure 12, the angular velocity of the two centrifugal blocks changes linearly with the change of time which is consistent with the effect of the set driving function, and the trend of the two centrifugal blocks' angular velocity is the same, and the angular velocities are both 1948.69deg/s, i.e.,

EXPERIMENTAL VALIDATION ANALYSIS

Experimental Design

From the above, if you want to realize the theoretical release speed of the DCSL, you need to set the corresponding DCSL parameters according to the parameters of the measuring wheel and the braking speed requirements of the car or cage. The experimental design of this paper is based on the mathematical model, the parameters of the measuring wheel and the braking speed requirements of the car or cage are consistent with the mathematical model in section 2, i.e. the center of mass of the measuring wheel is set at 4.8m/s, the diameter of the measuring wheel is 280mm, the release speed of the DCSL is 327.61r/min, and the range of error in the braking speed between the value of the mathematical model and the experimental data is 0~10%.

The single centrifugal block is made of 304 stainless steel, with a mass of 0.6 kg. The SRS is made of LC043EF15S316 of Lee Spring Co., Ltd, with a spring specification of 316 stainless steel, wire diameter of 1.09 mm, external diameter of 9.91 mm, free length of 50.8 mm, spring stiffness of 1.218 N/mm, and the two ends of the spring are closed and ground flat. Hydraulic sensor preload spring Lee Spring Co., Ltd's LC080L08S316, spring specification material for the 316 stainless steel, wire diameter 2.03mm, OD 24.64mm, free length of 63.5mm, spring stiffness 2.305N/mm, both ends closed and ground flat. Trigger shaft compression spring selection Lee Spring Co., Ltd LC045H05S316, spring specification material for the 316 stainless steel, wire diameter 1.14mm, OD 15.24mm, free length of 31.75mm, spring stiffness 1.173N/mm, both ends closed and ground flat. To increase the range of DCSL to meet the requirements of more working conditions, query the mechanical design manual, according to the length of the

33.99rad/s, at 9.48s, which is the same as that of the angular velocity of the DCSL of the mathematical model, i.e., 34.29 rad/s. The braking rotational speed error between them is 0.87%, which meets the specified error requirements, so the simulation verifies that the mathematical model is valid.

installation space of the SRS, the SRS working pressure and height, and the limit of the height of the pressure and set the experimental range of adjusting the pre-compression of the SRS for the range of 0mm to 10mm and take the integer, a total of 10 groups of experiments, each group of experiments was measured under 11 different pre-compression of the SRS limiter A total of 10 sets of experiments were set up, and each set of experiments measured the release speed of the DCSL under 11 different pre-compression amounts of the SRS.

Experimental Platform Construction and Data Acquisition

The experimental location is selected in a factory plant, and the experimental platform consists of a hydraulic sensor, a hydraulic sensor preloading spring device, and a DCSL integrated detection stage to collect the DCSL release speed under different SRS pre-compression amounts. The DCSL experimental detection diagram is shown in Figure 13.



Fig. 13. Experimental test chart of DCSL.

The electronic sensor adopts a QS-05N type proximity switch (NPN normally closed) sensor. The hardware test system is installed in the DCSL integrated test bench, in which the programmable controller adopts Mitsubishi FX5U-32MR/ES, which is connected to the encoder for real-time data acquisition through the input and output interfaces; the motor adopts 60 servo motors, and the servo drive adopts PS100 servo drive; the rotary encoder adopts

E6B2-CWZ6C OMRON with a pulse rate of 1024PPR. The incremental encoder with a pulse rate of 1024 PPR and a speed range of 0~3000r/min is used to detect the

real-time speed of the DCSL. The hardware connection diagram of this test system is shown in Figure 14.

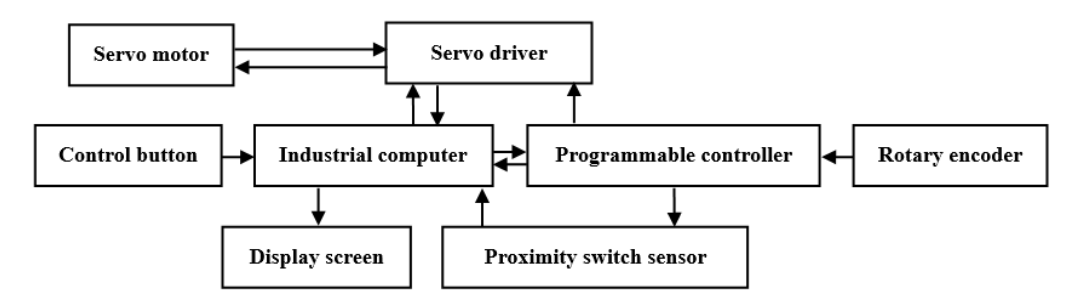


Fig.14. Hardware connection of the control system.

The DCSL is mounted in the same way as in the actual application, i.e. as a cantilever, without any support mount at the bottom. The DCSL is mounted on the output shaft of the motor of the centrifugal releaser integrated test bench to realize the function of the speed wheel to drive the DCSL to rotate through the flat key connection. The height and position of the hydraulic sensor preload spring unit frame are adjusted so that the push rod contacts the DCSL trigger shaft. Pre-tensioning spring device is installed at the left end of the hydraulic sensor, hydraulic sensor to realize the function of the hydraulic valve, that is, when the DCSL is in normal operation, the distance between the sensor and the pre-tensioning spring is very small, the pretensioning spring is compressed and leave a certain amount of tension, the sensor has no signal fluctuations, and then do not act to keep the function of the normally closed. When the DCSL speed reaches the set release speed, the centrifugal block under the action of centrifugal force away from the center of the axis swings outward, the T-plate and then out of the trigger shaft slot position, because the hydraulic sensor preload spring preload force is greater than the trigger shaft compression spring compression force, so the

preload spring stretching and push rod to promote the trigger shaft, the trigger shaft is released and axially to the DCSL inside the movement of hydraulic sensors sensed the loss of signal! The analog hydraulic valve opens, the servo motor stops through the programmable controller, and the analog hydraulic braking system is activated to quickly stop the car or cage.

Set the parameters of the centrifugal release integrated test bench, so that the motor speed from 0r/min to start uniformly accelerated rotation, the upper limit is not set, to be able to detect the speed of the DCSL release speed under different SRS precompression amount. After each test is completed and the value is recorded in the book, the hydraulic sensor preload spring position needs to be manually reset to the hydraulic sensor signal light is on, the trigger shaft will be automatically reset under the action of the spring force of the compression spring of the trigger shaft; manually reset the centrifugal block and the Tplate, and calibrate the T-plate in the correct position in the card slot, to ensure that the accuracy and rigor of the experiments. The experimental data are shown in Table 3.

Table 3. Experimental data table.

Pre-	DCSL release speed (r/min)									
compression (mm)	Group 1	Group 2	Group 3	Group 4	Group 5	Group 6	Group 7	Group 8	Group 9	Group 10
0	310.08	310.80	310.56	310.56	310.56	310.56	309.36	310.32	310.08	310.32
1	323.28	324.24	323.76	327.60	323.76	324.00	324.00	330.16	324.00	324.00
2	334.32	336.72	338.16	334.80	336.48	334.08	334.80	336.72	336.96	333.36
3	351.12	353.52	353.52	353.76	353.28	353.28	353.04	351.12	349.68	353.52
4	362.16	361.20	360.96	361.44	361.20	361.20	360.72	360.96	361.20	361.20
5	373.20	372.96	374.64	372.48	371.28	372.96	372.72	371.76	372.48	372.72
6	385.20	387.00	384.00	384.24	384.24	383.52	385.76	385.72	386.24	386.96
7	397.08	394.32	391.44	391.44	394.24	392.16	396.88	394.44	390.96	395.40
8	405.92	402.00	402.24	401.76	402.00	403.44	406.32	406.88	406.00	407.16
9	414.56	414.48	411.12	418.02	418.64	410.40	409.20	408.72	415.08	416.60
10	427.20	425.76	430.56	429.76	428.72	424.56	422.64	418.80	428.24	429.28

Analysis of Experimental Data

As can be seen from Table 3, when the adjusting nut is adjusted so that the SRS pre-compression is 2mm, **DCSL** release rotational speed 333.36~338.16r/min, and the error between the DCSL release rotational speed of 327.61r/min required by the working conditions is 1.76%~3.22%, which is all in the specified error range of braking rotational speed, therefore, the mathematical model for the DCSL in section 2 Therefore, the mathematical model of the DCSL in section 2 can meet the set working conditions and the mathematical model is reasonable, and the errors between the mathematical model values and the experimental values are within the specified error range.

Because the total number of experiments and data in this paper is large, and the DCSL release speed of the same SRS pre-compression under different subgroups is different, and there is a transverse gap in the numerical value, therefore, to verify the mathematical model more intuitively and to facilitate the comparison with the theoretically calculated value, the above experimental data should be processed by mathematical modeling, to fit a unique value of experimental data that can represent the precompression of different SRS.

DATA PROCESSING AND VALIDATION

Data Processing

Assuming that the above ten sets of experimental data as independent variables, each set of experimental data is a separate independent variable, it is clear that the number of independent variables is greater than two; and for each pre-compression amount of the number of experiments detected by the limited number of experiments, experimental values are different, the most representative of the pre-compression amount of the value cannot be determined, therefore, regression analysis can be used in the multiple linear regression, multiple linear regression through the fit a set of independent variables affected by the independent variables and linear synthesis of the dependent variable, that is, the desired unique experimental value that can represent each pre-compression amount. Therefore, multiple linear regression in regression analysis can be used to fit a set of dependent variables that are linearly synthesized by these independent variables, i.e., the desired unique experimental values that can represent each pre-compression amount(Gao Ji-Wen, 2023). A phenomenon is often associated with multiple factors, and the optimal combination of multiple independent variables together to predict or estimate the dependent variable is more effective and realistic than using only one independent variable for prediction or estimation.

First, the scatterplot of each group of experimental data was drawn in MATLAB software to analyze the experimental data, and the scatterplot of the experimental data is shown in Fig. 15

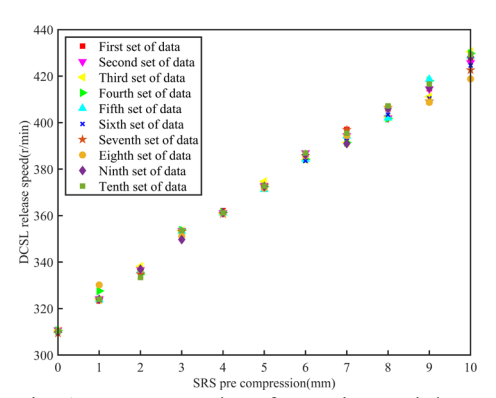


Fig. 15. Scatter plot of experimental data.

It can be seen intuitively from the above figure that the DCSL release speed of each group of experimental data increases linearly with the increase of the pre-compression of the SRS. Therefore, each group of experimental data is linearly changing, it can be seen that these ten groups of experimental data can be linearly synthesized into a set of experimental values that can represent the amount of each pre-compression.

The reliability of the experimental values fitted by the multiple linear regression with the experimental data curves is considered comprehensively by setting the significance level = 0.05 i.e. 95% confidence interval, regression coefficient estimates and their confidence intervals, residuals and their confidence intervals, test regression model statistics i.e. goodness-of-fit \mathbf{R}^2 , the \mathbf{F} -tests of overall significance test of the equations, \mathbf{P} -values, and the estimates of the error variance (Brown, 2009). Therefore, the above test parameters were programmed in MATLAB to produce the experimental values calculated by multiple linear regression as shown in Table 4.

Table 4. Data table for multiple linear regression fitting

fitting.			
Pre-compression (mm)	Fitted release speed (r/min)		
0	309.81		
1	323.26		
2	334.41		
3	351.48		
4	362.70		
5	372.46		
6	385.47		
7	396.89		
8	405.96		

9	414.34
10	427.34

As can be seen from Table 4, the fitted data obtained from the multiple linear regression is close to the first set of experimental data, and because the goodness of fit $R^2 = 0.99992$ means that 99.992% of the dependent variable can be determined from the experimental data, i.e., the unique experimental value that can represent each pre-compression amount synthesized by the joint influence of ten sets of experimental data can be determined by the measured experimental data; the value of 1 is far more than the critical value of the 2-test, and the value of 3 is far less than the critical value of 2-test, thus the regression model is reliable as a whole. The value of F is much more than the critical value of the F -test, P is much less than α , and thus the regression model is reliable as a whole. Figure 16 shows a graph of the experimental data.

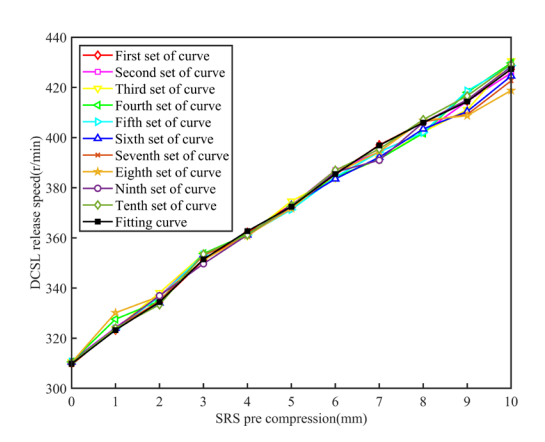


Fig. 16. Graph of experimental data.

From the above figure, it can be seen that the multiple linear regression fitted curves are close to the experimental data curves with not much error, and because the results of the above test parameters all indicate that the fitted data are accurate and reliable, the data fitted by the multiple linear regression can be used as the only experimental value representing each pre-compression in the experiment.

Validation of the Mathematical Model

In the previous subsection, the experimental data have been processed by regression analysis to fit a unique set of experimental values that are representative of each pre-compression amount and that are reliable. In the second section, the theoretical release speed of the DCSL with different pre-compressions of the SRS has been calculated by Equation (31) when the operating conditions and parameters of the DCSL have been set, so this section

should further verify whether the reliability of the DCSL action is closer to reality, i.e., whether the braking speed error between the theoretical release speed of the DCSL and the experimental release speed is within the specified error range of 10%. The comparison between the mathematical model values and the experimental values is shown in Table 5.

Table 5. Comparison of theoretical calculated and experimental values.

Pre- compression (mm)	Theoretical release speed (r/min)	Experimental release speed (r/min)
0	287.38	309.81
1	310.37	323.26
2	331.77	334.41
3	351.87	351.48
4	370.88	362.70
5	388.96	372.46
6	406.24	385.47
7	422.82	396.89
8	438.77	405.96
9	454.16	414.34
10	469.04	427.34

From the above table, it can be seen that the numerical difference between the theoretically calculated release rotational speed and the linearly synthesized release rotational speed of the experimental data under different SRS precompressions is not significant, and the braking rotational speed error between the experimental release rotational speed and the theoretical release rotational speed ranges from 0.11% to 8.89%, which are all in the specified error range, so the experimental validation of the mathematical model is established.

CONCLUSIONS

- (1) This paper establishes the triggering model of the DCSL through kinetic analysis and carries out MATLAB simulation calculation on the triggering model, which concludes that the triggering system of the DCSL meets the characteristics of the SRS stiffness and the pre-compression of the SRS, and the larger the pre-compressed amount of the SRS, and the smaller the total mass of the centrifugal block is, then the larger the DCSL releases.
- (2) The mathematical model of the DCSL is derived by setting the working conditions and parameters of the DCSL, and the kinetic simulation analysis of the mathematical model is carried out by using ADAMS to derive the braking rotational speed error between the simulated releasing rotational speed

- and the target releasing rotational speed to be 0.87%, and the reliability of the mathematical model. According to the mathematical model to design the experiment, build the experimental platform and hardware testing system, using scientific experimental methods to collect data, it is concluded that when the pre-compression of the SRS is 2mm can meet the requirements of the working conditions, the braking speed error is 1.76%~3.22%, within the specified error range.
- (3) The use of MATLAB for mathematical modeling of the experimental data collected on-site, the error between the mathematical model value and the experimental value is 0.11%~8.89%, which is within the specified error range, and the experiment verifies that the mathematical model is established. The research results of this paper can effectively solve the current technical problems of the centrifugal DCSL, the speed limit range is wide, to meet the requirements of more working conditions, for the actual centrifugal DCSL design selection, and drive control to provide a reliable reference basis.

REFERENCES

- Brown S H. "Multiple linear regression analysis: a matrix approach with MATLAB[J]." *Alabama Journal of Mathematics*, 2009, 34: 1-
- "Circular of the General Administration of Market Supervision on the Safety Condition of National Special Equipment in 2022[J]."

 China Special Equipment Safety, 2023, 39(03):1-3.
- Chen, X., & Li, X. (2016, April). "Android-based noncontact elevator overspeed governor speed measuring system." In 2016 3rd International Conference on Mechatronics and Information Technology (pp. 67-71). Atlantis Press.
- DING Caihong, WANG Zhanyong, WANG Yongliang et al. "Analysis of the current situation and inspection requirements of elevator car upward overspeed protection device[J]." *China Special Equipment Safety*, 2021, 37(02):22-26.
- Gao Ji-Wen. "Estimation of multiple linear regression parameters[J]." *Journal of Xi'an College of Arts and Sciences (Natural Science Edition)*,2023,26(03):1-5+12.
- Gao, J., Teng, Y. F., & Yuan, W. C. (2014). "Applied Technology the test of elevator running mileage (dynamic) of scientific significance." Advanced Materials Research, 1022, 277-281.
- Li Jun. "Discussion on the design and calculation of centrifugal block type speed limiter for elevator[J]." *China Elevator*,2020,31(13):32-34.
- LI Wanli, BIAN Kaite. "Theoretical and experimental study on the triggering of two-way speed

- limiter for elevator[J]." China Journal of Construction Machinery, 2017, 15(05): 377-382.
- M. J. Gradziel & K. J. "Holgerson: Aerospace Conference," 2008 IEEE (March 1-8, 2008), p.1-20.
- Peng, T. J., Kuo, P. H., Huang, W. C., & Wang, C. C. (2024). "Nonlinear Dynamic Analysis and Forecasting of Symmetric Aerostatic Cavities Bearing Systems." *International Journal of Bifurcation and Chaos*, 34(04), 2430008.
- Prahlow, J. A., Ashraf, Z., Plaza, N., Rogers, C., Ferreira, P., Fowler, D. R., ... & Lantz, P. E. (2020). "Elevator-related deaths." *Journal of forensic sciences*, 65(3), 823-832.
- Shuangchang, F., Jie, C., Yanbin, Z., & Zheyi, L. (2020, October). "Discussion on improving safety in elevator management." In 2020 2nd International Conference on Machine Learning, Big Data and Business Intelligence (MLBDBI) (pp. 195-198). IEEE.
- Shuangchang, F., Jie, C., & Xiaoqing, C. (2020, May). "Analysis of the hidden danger for old elevator safety." In 2020 3rd International Conference on Electron Device and Mechanical Engineering (ICEDME) (pp. 605-608). IEEE.
- Vermalle J C: "14th Aerospace Mechanisms Symposium:" proceedings of a symposium held at NASA Langley Research Center (Hampton, Virginia, USA, May 1-2, 1980.), 2127: 93.
- Wang, C., & Feng, S. (2020, July). "Research on collection and preprocessing of multisource heterogeneous elevator data." In 2020 IEEE international conference on power, intelligent computing and systems (ICPICS) (pp. 490-493). IEEE.
- Wang, C. C., Kuo, P. H., Peng, T. J., Oshima, M., Cuypers, S., & Chen, Y. T. (2024). "Voting model prediction of nonlinear behavior for double-circumferential-slot air bearing system." *Chaos, Solitons & Fractals, 183,* 114908.
- Yanbin, Z., Shangchang, F., Zheyi, L., & Kuangye, N. (2020, October). "The statistics and analysis of annual fault repair report of an elevator company." In 2020 2nd International Conference on Machine Learning, Big Data and Business Intelligence (MLBDBI) (pp. 576-579). IEEE.
- Yang, G., & Liang, H. (2015). "Condition monitoring and fault diagnosis for an antifalling safety device." Shock and Vibration, 2015(1), 286781.
- Zhang Shuai. "Dynamic modeling and ADAMS simulation analysis of a six-axis assembly robot[J]." *Mechanical Engineering and Automation*, 2024, (02):47-49+52.

NOMENCLATURE

 a_n normal acceleration

 a_{τ} tangential acceleration

 F_f friction between the tail part of the T-plate and the trigger shaft

 F_{k1} the compression force of the SRS

 F_{k2} the compression force of the SRS

 F_{k3} the preload force of the hydraulic sensor preload spring acting on the outer face of the trigger shaft

 F_{k4} the trigger shaft compression spring compression force acting on the inner end face of the trigger shaft

 F_n the normal centrifugal force

 F_P the positive pressure between the end of the T-plate lever and the trigger shaft

 F_{pm1} the positive pressure of the guide rod on the centrifugal block A

 F_{pm2} the positive pressure of the guide rod on the centrifugal block B

k the spring stiffness of the SRS

 k_3 the spring stiffness of the hydraulic sensor preload spring

 k_4 the trigger shaft compression spring stiffness

 L_1 the free length of the SRS

 L_2 the length of the installation space of the SRS

N SRS to preload the centrifugal block

r the distance from the center of the DCSL shaft to the center of mass of the centrifugal block when the DCSL is not triggered

R the distance from the center of the DCSL shaft to the center of mass of the centrifugal block when the DCSL is released from the trigger shaft

 R_1 the radius of the speed wheel

 v_0 the linear velocity of the centrifugal block center of

 v_{cri} the critical linear velocity of the trigger shaft by the release of the DCSL

V the center-of-mass velocity of the speed wheel

 x_0 the pre-compression amount of the SRS

 x_1 the compression amount of the SRS

 x_3 the hydraulic sensor preload spring total compression

 x_4 the trigger shaft compression spring total compression

 μ the friction coefficient between the end of the T-

plate lever and the trigger shaft

 ω the angular speed of the speed wheel

 ω_i the angular speed of the DCSL